

Low temperature fused deposition modelling (FDM) 3D printing of thermolabile drugs

Gayathri Kollamaram¹, Denise M. Croker¹, Gavin M. Walker¹, Alvaro Goyanes^{2*} Abdul W. Basit^{2, 3}, Simon Gaisford^{2, 3*}

¹ Synthesis & Solid State Pharmaceutical Centre (SSPC), Department of Chemical Sciences, Bernal Institute, University of Limerick, Limerick, Ireland.

² FabRx Ltd., 3 Romney Road, Ashford, Kent TN24 0RW, UK.

³ UCL School of Pharmacy, University College London, 29-39 Brunswick Square, London WC1N 1AX, UK.

*Correspondence: Simon Gaisford - s.gaisford @ucl.ac.uk

Alvaro Goyanes - a.goyanes@FabRx.co.uk

Abstract

Fused deposition modeling (FDM) is the most evaluated 3D printing technology for the manufacture of personalized medicines in the pharmaceutical field however high temperatures associated with the process limit its application. The objective of this study was to lower the FDM printing temperature to accommodate low-melting and thermolabile drugs. Immediate release polymers Kollidon VA64 and Kollidon 12PF were investigated as the potential candidates for low-temperature FDM printing using ramipril as the model drug with low melting point (109°C). Filaments loaded with 3% drug were obtained by hot melt extrusion at 70°C and printed at 90°C - the lowest temperature reported so far to the authors' knowledge. Ramipril printlets with a dose equivalent of 2 mg were printed and HPLC results showed no drug degradation. Results from dissolution studies showed that 100% drug release was achieved within 30 min. Variable temperature Raman and solid-state nuclear magnetic resonance (SSNMR) spectroscopy techniques were used to evaluate drug stability over the processing temperature range. The data indicated that ramipril did not undergo degradation below its melting point (which is above the processing temperature range: 70 – 90 °C) but was transformed into the impurity diketopiperazine following exposure to temperatures higher than its melting point. The use of these excipients in FDM printing was further validated by printing with the drug 4-aminosalicylic acid (4-ASA), which in previous work was reported to undergo degradation in FDM printing. However, it was 4-ASA was found to be stable in the current study. This work demonstrates that the selection and use of new excipients can overcome drug degradation problems in FDM printing making this technology suitable for drugs with lower melting temperatures.

Keywords:

Three-dimensional printing; Rapid prototyping; Additive manufacturing; Personalised medicines; Immediate release

1. Introduction

3D printing techniques have come a long way since their inception in early '90s when they were developed for rapid and economic production of prototype models (Sachs et al., 1993) and now further applied in biomanufacturing (Chia and Wu, 2015) and pharmaceuticals (Alomari et al., 2015; Trenfield et al., 2018). The importance and relevance of 3D printing technologies for pharmaceutical applications have been extensively discussed elsewhere (Alhnan et al., 2016; Palo et al., 2017) as an enabling technology to produce patient-tailored medicines (Pietrzak et al., 2015), to engineer drug release profiles from a dosage form (Fina et al., 2017; Goyanes et al., 2015d) and to deliver multiple drugs (Khaled et al., 2015a, b).

Fused deposition modelling (FDM) is the most evaluated of the 3D printing techniques in the pharmaceutical field owing to its relatively simpler and less-expensive equipment, diverse choice of excipients and ease of producing dosage forms with complex geometries which have greater patient compliance (Goyanes et al., 2015c; Goyanes et al., 2017; Schiele et al., 2013). FDM process involves heating and extruding a drug loaded polymer strand (previously prepared by hot melt extrusion) through a nozzle tip followed by solidification onto a build plate into the desired geometry. One potential issue with this type of printing therefore is the high temperature the drugs might be exposed to during material extrusion and printing. A previous study showed the thermal degradation of 4-aminosalicylic acid (4-ASA) during FDM reached 50%, emphasising the need for bringing down processing temperatures for thermally labile drugs (Goyanes et al., 2015a).

The majority of the existing literature on pharmaceutical applications of FDM involves printing temperatures in the range of 150-230°C, primarily using polyvinyl alcohol (PVA), polylactic acid (PLA), hydroxypropyl cellulose (HPC) and various grades of Eudragit polymers (RL, RS and E), since these polymers extrude and print well (Goyanes et al., 2014; Goyanes et al., 2015a; Goyanes et al., 2015c; Melocchi et al., 2015; Pietrzak et al., 2015; Skowrya et al., 2015). However, most of these polymers, excluding Eudragit E and HPC, are not well suited for formulation of immediate release dosage forms, which account for approximately 70% of oral dosage formulations (Okwuosa et al., 2016). There are limited studies investigating immediate release 3D printed formulations, using PVP and Eudragit EPO, that print at relatively lower temperatures in the range of 110-135 °C (Okwuosa et al., 2016; Sadia et al., 2016). There is therefore a need to develop polymer filaments that are; (i) suitable for immediate release formulations and; (ii) extrude and print at lower temperatures so as to enable 3D printing of thermolabile and low-melting point drugs.

Reports about the use of Kollidon VA64 and Kollidon 12PF in association with the plasticizer - PEG 1500 on the suitability of polymers for hot melt extrusion throws light on these polymer-plasticizer combinations, as potential candidates for exploring possible filament compositions that could be printed at significantly lower temperatures (Karl et al., 2010). Kollidon VA64 is a water soluble vinylpyrrolidone-vinyl acetate copolymer, widely used in pharmaceutical formulations as a direct compression, film-forming and taste-masking excipient and is known for its suitability in hot-melt extrusion processes. Kollidon 12PF is a low molecular grade polyvinylpyrrolidone commonly used as a solubilising agent and crystallization inhibitor.

A drug that could benefit from advances in lower printing temperatures is ramipril, an angiotensin converting enzyme (ACE) inhibitor antihypertensive agent, normally used in combination with other drugs in the treatment of multitude of cardiovascular indications. Ramipril has a melting point of 109 °C and requires dose flexibility. It is available in fixed dosage strengths ranging between 1.25 mg and 20 mg with an initial dose of 1.25 or 2.5 mg. Alternatively, ramipril may require dose adjustment depending on blood potassium levels and concurrent administration of diuretics (Warner and Perry, 2002).

The objective of the present work was to explore the use of Kollidon VA64 and Kollidon 12PF as suitable excipients to prepare immediate release formulations lowering the printing temperature of the FDM 3D printing process in order to accommodate thermolabile and low-melting drugs. Printlets (3D printed tablets) incorporating therapeutically relevant dose of ramipril (selected as a model drug) were prepared by FDM printing. Physical, chemical and solid-state properties and drug release profiles from the printlets were evaluated.

2. Material and Methods

Ramipril (RMP) was purchased from Baoji Guokang Bio Technology Co Ltd (Baoji, China). Kollidon VA64 (vinylpyrrolidone-vinyl acetate copolymers) and Kollidon 12PF (polyvinylpyrrolidone) were obtained from BASF (Germany), PEG 1500 and magnesium carbonate were purchased from Sigma Aldrich (UK), Mannitol was purchased from Alfa Aesar (UK), formic acid and analytical grades of acetonitrile and methanol, and 4-aminosalicylic acid (4-ASA) were purchased from VWR International Ltd., (UK).

2.1. Preparation of drug-loaded Kollidon filaments

Kollidon VA 64, PEG 1500, mannitol, ramipril and magnesium carbonate (65%, 20%, 10%, 3% and 2% w/w respectively) were manually mixed using a mortar and pestle (Table 1). The mixture was then extruded using a single-screw extruder (Noztek Pro filament extruder, Noztek, UK) at 70 °C through a nozzle with diameter 1.3 mm at screw speed of 15 rpm. The resulting filament was stored in a vacuum desiccator before printing. Ramipril loading in the filaments was determined by HPLC analysis. Filaments were also formulated by replacing 50% and 40% of Kollidon VA64 from the above formulation with Kollidon 12PF (Table 1).

2.2. 3D printing of ramipril dosage forms

Dosage forms were fabricated with the drug-loaded filament using a standard fused-deposition modelling 3D printer, MakerBot Replicator 2X Desktop (MakerBot Inc., USA). The template used to print the dosage form was designed with AutoCAD 2014 (Autodesk Inc., USA) and exported as a stereolithography (.stl) file into MakerWare v. 2.4.1 (MakerBot Inc., USA). The selected geometry of the dosage forms was a flat faced cylindrical tablet with dimensions, X = 10 mm, Y = 10 mm and Z = 3.6 mm. The infill percentage was 100% in order to produce solid dosage forms of high density and other printer settings were as follows: standard resolution with the raft option deactivated and an extrusion temperature of 90 °C, speed while extruding (90 mm/s), speed while traveling (150mm/s), number of shells (2) and layer height (0.20 mm).

Table 1. Composition of the formulations

Formulation	Ramipril (%)	Magnesium carbonate (%)	Mannitol (%)	PEG 1500 (%)	Kollidon VA64 (%)	Kollidon 12 PF (%)	Extrusion temperature (°C)	Printing temperature (°C)
VA64	3	2	10	20	65	-	70	90
VA64:12PF (3:2)	3	2	10	20	39	26	65	90
VA64:12PF (1:1)	3	2	10	20	32.5	32.5	65	90

2.3. Morphology

The physical dimensions of the printlets were measured using a digital Vernier caliper. Pictures of the devices were taken with a Nikon Coolpix S6150 with the macro option of the menu.

2.4. Determination of the mechanical properties of the printlets

The printlet breaking force of 6 printlets of each type was measured using a traditional tablet hardness tester TBH 200 (Erweka GmbH, Heusenstamm, Germany), whereby an increasing force is applied perpendicular to the tablet axis to opposite sides of a tablet until the printlet fractures.

2.5. X-ray Powder Diffraction (XRPD)

X-ray powder diffraction data were obtained using Cu-K α ($\lambda = 1.5418 \text{ \AA}$) radiation with a Philips PANalytical X'Pert MPD Pro diffractometer (with PW3064 sample spinner and PANalytical Data Collector) operating at 40 kV. X-ray measurements were collected over a 2θ range of $5\text{--}40^\circ$ with a step size of 0.007° and scan step time of 60s. The resulting diffractograms were analysed using PANalytical High Score plus against the standard references from the Cambridge structural database.

2.6. Thermal Analysis

Differential scanning calorimetry (DSC) and thermogravimetric analysis (TGA) were used to characterise the melting point and degradation profile of the drug. DSC measurements were performed with a Q2000 DSC (TA Instruments, Waters, LLC, U.S.A.) at a heating rate of $10^\circ\text{C}/\text{min}$. Calibration for cell constant and enthalpy was performed with indium ($T_m = 156.6^\circ\text{C}$, $\Delta H_f = 28.71 \text{ J/g}$) according to the manufacturer instructions. Nitrogen was used as a purge gas with a flow rate of $50 \text{ mL}/\text{min}$ for all the experiments. Data were collected with TA Advantage software for Q series (version 2.8.394), and analysed using TA Instruments Universal Analysis 2000. Melting temperature is reported as extrapolated onset unless otherwise stated. TA aluminium pans and lids (Tzero) were used with an average sample mass of $8\text{--}10 \text{ mg}$. For TGA analysis, samples were heated at $10^\circ\text{C}/\text{min}$ in open aluminium pans with a Discovery TGA (TA Instruments, Waters, LLC, U.S.A.). Nitrogen was used as a purge gas with a flow rate of $25 \text{ mL}/\text{min}$. Data collection and analysis were performed using TA Instruments Trios software and percent mass loss or onset temperature were calculated

2.7. Determination of Drug Loading

A printlet or a section of drug-loaded strand (approximately 1g) was placed in a volumetric flask with deionized water (1 L) under magnetic stirring until complete dissolution ($n = 3$). Samples of the solutions were then filtered through 0.45 μm filter (Millipore Ltd., Ireland) and the concentration of drug determined with HPLC (Hewlett-Packard 1050 Series HPLC system, Agilent Technologies, U.K.).

For ramipril, the validated high performance liquid chromatographic assay entailed, injecting 5 μL samples for analysis using a mobile phase, consisting of isocratic system of aqueous phase (10%) composed of 0.1% formic acid and organic phase (90%) composed of methanol and acetonitrile (15:85) pumped at a flow rate of 1 mL/min, through a Luna 5 μm C18 column, 150 x 4.6 mm (Phenomenex, U.K.) maintained at 40 °C. The eluent was screened at a wavelength of 210nm. The assay method for ramipril was proven to be discriminatory for the impurity ramipril diketopiperazine (impurity D), the anticipated inactive degradant of ramipril. Impurity D was prepared as per the method given by (Amjad Anwwari, 2008). Retention times of ramipril and the impurity D were found to be 2.4 and 6.1 min respectively. All measurements were made in duplicate.

For 4-ASA, the HPLC method involved injecting 10 μL samples for analysis using a mobile phase, consisting of isocratic system of aqueous phase (76%) composed of 0.1% orthophosphoric acid and organic phase (24%) composed of acetonitrile pumped at a flow rate of 1 mL/min through a Discovery HSF5 column (4.6 \times 150 mm) maintained at 40 °C. The eluent was screened at a wavelength of 303 nm and all measurements were made in duplicate.

2.8. Dissolution testing

Dissolution profiles were obtained using a USP-II apparatus (Model PTWS, Pharmatest, Germany). In each assay, the printlets were placed at the bottom of the vessel in 0.1N HCl pH 1.2, (750 mL) under constant paddle stirring (50 rpm) at 37 °C. During the dissolution test, samples of ramipril were automatically removed and filtered through 10 μm filters and drug concentration was determined using an in-line UV spectrophotometer (Cecil 2020, Cecil Instruments Ltd., Cambridge, UK) operated at the wavelength of maximum absorbance of the drug in 0.1N HCl (210 nm). Data were processed using Icalis software (Icalis Data Systems

Ltd., Berkshire, UK). Tests were conducted in triplicate under sink conditions. Data are reported throughout as mean \pm standard deviation.

2.9. Raman Spectroscopy

Raman spectroscopy was carried out using a LabRAM HR Evolution (HORIBA UK Ltd.) in a backscatter configuration with 532 nm excitation (laser power 499 mW), and an acquisition time of 10 s for 3 accumulations. Spectra were collected using a 50X objective at a 4 cm^{-1} resolution, over scan ranges of 50 to 3400 cm^{-1} using 600 gr/mm grating. For the spectra collected in z-axis, 100X objective was used with a step size of 1 μm . Variable temperature experiments were conducted using a hot stage associated with the spectrometer. Samples were heated at 10 $^{\circ}\text{C}/\text{min}$ and held for 5 min at specific temperature while spectra were collected.

2.10. Solid-state nuclear magnetic resonance (SSNMR) spectroscopy

Solid-state NMR data were acquired on a Bruker Avance III HD wide bore NMR spectrometer operating at a static magnetic field strength of $B_0 = 9.4$ T. Powdered or granular samples of ramipril, ramipril diketopiperazine, extruded filament, and a physical mixture of the compounds comprising the extruded filament were packed into 4 mm o.d. zirconia rotors with either Kel-F or zirconia caps. Carbon-13 NMR spectra were acquired under magic angle spinning (MAS) conditions using a Bruker 4 mm triple resonance (X/Y/ ^1H) MAS probe operating in double resonance mode. Spectra were acquired at ^{13}C and ^1H Larmor frequencies of $\nu_0 = 100.6$ and 400.1 MHz, respectively, and processed using TopSpin version 3.5p17. NMR spectra were acquired at temperatures between 20 and 90 $^{\circ}\text{C}$. The sample temperature in variable temperature NMR experiments was controlled with a BVTB 3500 temperature control unit operated via the TopSpin software. The heating rate was limited to a maximum of 5 $^{\circ}\text{C}/\text{min}$.

Carbon-13 NMR spectra were collected using a cross polarization (CP) pulse sequence with total suppression of spinning sidebands (TOSS) (Antzutkin, 1999; Song et al., 1993). Proton 90 degree pulses were 3 μs in length, and ^{13}C 90 and 180 degree pulses were 4 and 8 μs in length, respectively. Samples were spun at MAS rates of 6 or 12 kHz. Proton decoupling at a frequency of 83 kHz was carried out using the SPINAL64 (Fung et al., 2000) decoupling sequence. Proton T_1 values were determined using the saturation recovery pulse sequence and recycle delays were an optimized $1.3 \cdot T_1$ for each sample at each temperature except where short recycle delays were prohibited by the duty cycle. Recycle delays varied from 3.5 to 5 s

for ramipril, 3.5 s for ramipril diketopiperazine, and were 10 s for the filament and the physical mixture of compounds. Contact times in CP experiments were optimized for bulk crystalline ramipril and were 2 ms. The number of transients obtained for the ^{13}C NMR spectra of ramipril and ramipril diketopiperazine ranged from 243 to 1944; 7290 transients were averaged for the ^{13}C NMR spectra of the filament and physical mixture of compounds. Carbon-13 chemical shift values were referenced to TMS at $\delta = 0$ ppm by adjusting the field such that the methylene peak in the ^{13}C NMR spectrum of solid adamantane resonated at $\delta_{\text{iso}} = 38.48$ ppm (Morcombe and Zilm, 2003). For all ^{13}C NMR spectra, 10 Hz of line broadening was applied before processing.

Sample temperatures under MAS conditions were calibrated using ^{207}Pb NMR spectra of solid powdered lead(II) nitrate (Bielecki and Burum, 1995; Takahashi et al., 1999). The temperature at ambient conditions was determined using a sample of neat methanol (Ammann et al., 1982). Lead-207 NMR data were acquired using single-pulse experiments with a 4 μs 90 degree pulse at a Larmor frequency of 83.4 MHz. The recycle delay and number of transients in ^{207}Pb NMR spectra were 60 s and 16 transients, respectively.

Plots of NMR spectra were prepared for publication with DMFit (Massiot et al., 2002).

3. Results and discussion

Ramipril printlets were successfully printed by FDM 3D printing (Figure 1) for all the formulations listed in the Table 1; printing at 90 °C is the lowest ever temperature reported so far to the authors' knowledge. The printlets produced were white colour and showed a good uniformity of physical dimension with a mean thickness of 3.62 ± 0.05 mm, 10.54 ± 0.04 mm diameter and weight of 294.5 ± 3 mg.



Figure 1. Image of ramipril printlets. From left to right: VA64, VA64:12PF (3:2) and VA64:PF12 (1:1)

All formulations show appropriate properties for handling and were mechanically strong. The printlet breaking force data show values close to 485 N which represent the maximum value measurable by the tablet hardness tester. These values are comparable to those previously reported from printlets prepared using polyvinyl alcohol (PVA) (Goyanes et al., 2015b).

The immediate release polymers Kollidon VA 64 and Kollidon 12PF were found to be viable excipients for printing at temperatures below 100 °C. Initially ramipril loaded filaments were produced using Kollidon VA64 alone as the polymer without any Kollidon 12PF, in combination with PEG 1500 as a primary plasticizer, mannitol, and magnesium carbonate as a stabilising agent. Mannitol was added as a secondary plasticizer to produce filaments with sufficient flexibility for printing and additionally for its pore former capacity as mannitol has previously been reported as a channelling agent in 3D printed formulations (Beck et al., 2017). Magnesium carbonate is a pharmaceutically accepted excipient, which has been reported to have a stabilizing effect on ACE inhibitors in a formulation by providing an alkaline environment that protects the active ingredient from oxidation, hydrolysis and cyclization (Harris et al., 1988), and is also known for its application in high temperature insulating compositions (Farrar, 1994). Numerous formulations were tested with varying polymer and plasticizer combinations (data not shown) in order to achieve filaments that could be produced at lower temperatures and that also had a good balance between flexibility and tensile strength so as to avoid collapsing and breaking during printing. The first selected formulation (VA64 from Table 1) was processed by hot melt extrusion at 75 °C to obtain the filament, used to print the cylindrical printlets (Figure 1) at 90 °C. A die with a diameter of 1.3 mm was used for extruding filaments of 1.75 mm diameter required for printing as the formulation expanded after exiting the nozzle of the extruder.

It is of the utmost importance to demonstrate the stability of the ramipril during extrusion and printing steps, considering its susceptibility to a range of factors such as mechanical stress, heat, moisture and excipients (Shafiq and Shakeel, 2008). DSC and TGA data were used to determine the melting point and degradation profile of the drug. These analytical methods indicated that the melting point of ramipril was 109 °C (Figure 2) and thus, further contributes to the need for printing the drug at lower temperature. Although the reduction in mass from the TGA is not observed until exposure to higher temperatures (130 °C), ramipril

is not stable below its melting point and transforms to ramipril diketopiperazine (impurity D) (Amjad Anwwari, 2008).

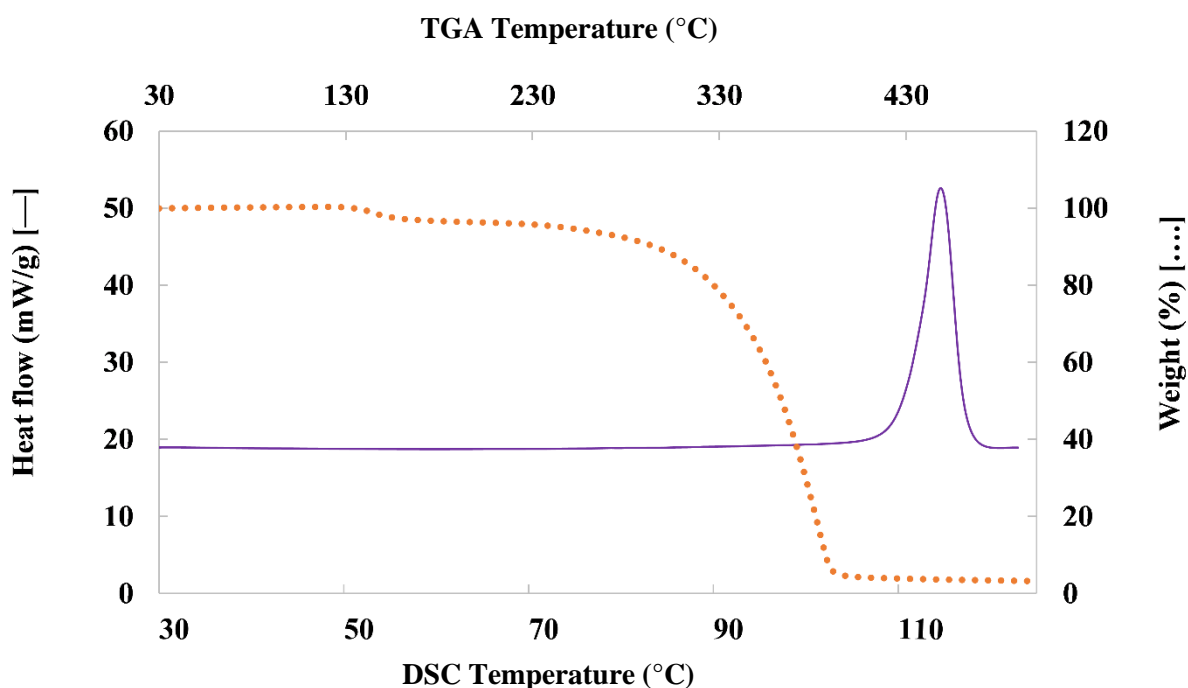


Figure 2. DSC and TGA plots of ramipril

Chemical integrity of the drug in the final printlets and drug-loaded filaments was analysed using HPLC; the drug loading of the filaments was $3.03 \text{ wt}\% \pm 0.04$ (theoretical loading- 3 wt%) and in the printlets was $1.98 \pm 0.03 \text{ mg}$ (theoretical amount- 2 mg), indicating no drug degradation. The stability of the drug over the processing temperature range was further confirmed using variable temperature Raman and SSNMR studies. Ramipril was analysed using a Raman spectrometer equipped with a hot stage microscope over a temperature range between 20 °C and 109 °C (melting point). The sample was analysed for any degradation by evaluating the Raman spectra collected, at room temperature, at 70 °C, the extrusion temperature and at 90°C, the printing temperature, Figure 3.

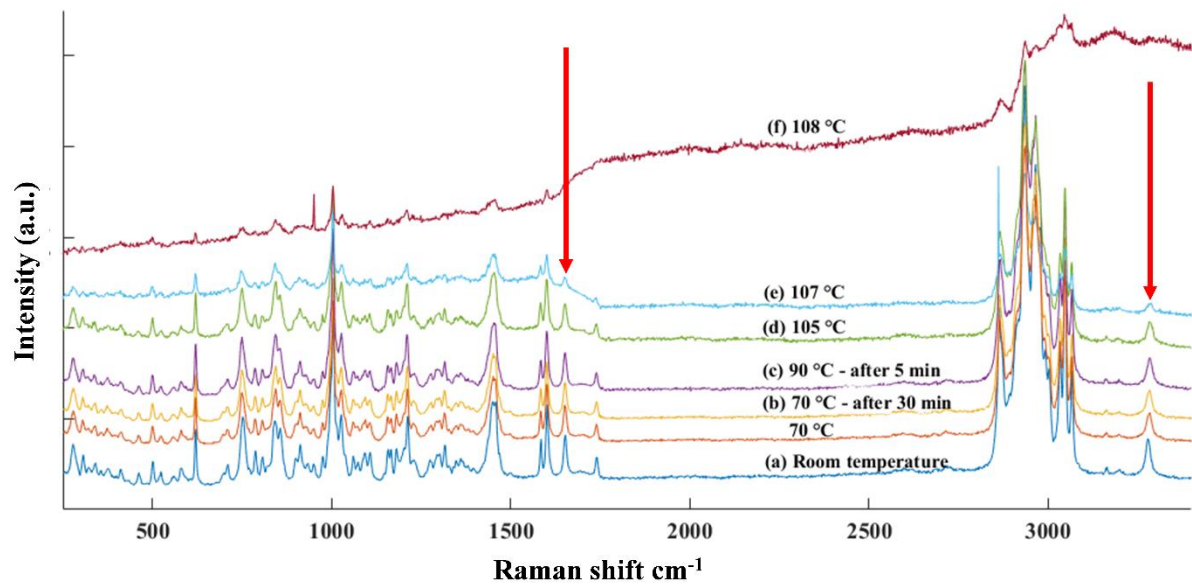


Figure 3. Raman spectra of ramipril collected at different temperatures (a) at room temperature, (b) at 70 °C after 30 min, (c) at 90 °C after 5min, (d) at 105 °C, (e) at 107 °C, (f) at 108 °C, corresponding to images in the Figure 3.

The drug was exposed to a specific temperature for a longer time during the extrusion than the printing process. Taking this into consideration ramipril was held at 70 °C for 30 min and at 90 °C for 5 min on a hot stage microscope, emulating longer exposure times to the temperatures during the extrusion and printing steps. It is evident from the spectral data (Figure 3) and micrographs (Figure 4) that ramipril did not undergo any degradation under these temperatures. Hence, ramipril is expected to be stable in the formulations which are composed of 97% excipients, thereby exhibiting an additional insulating effect on the drug.

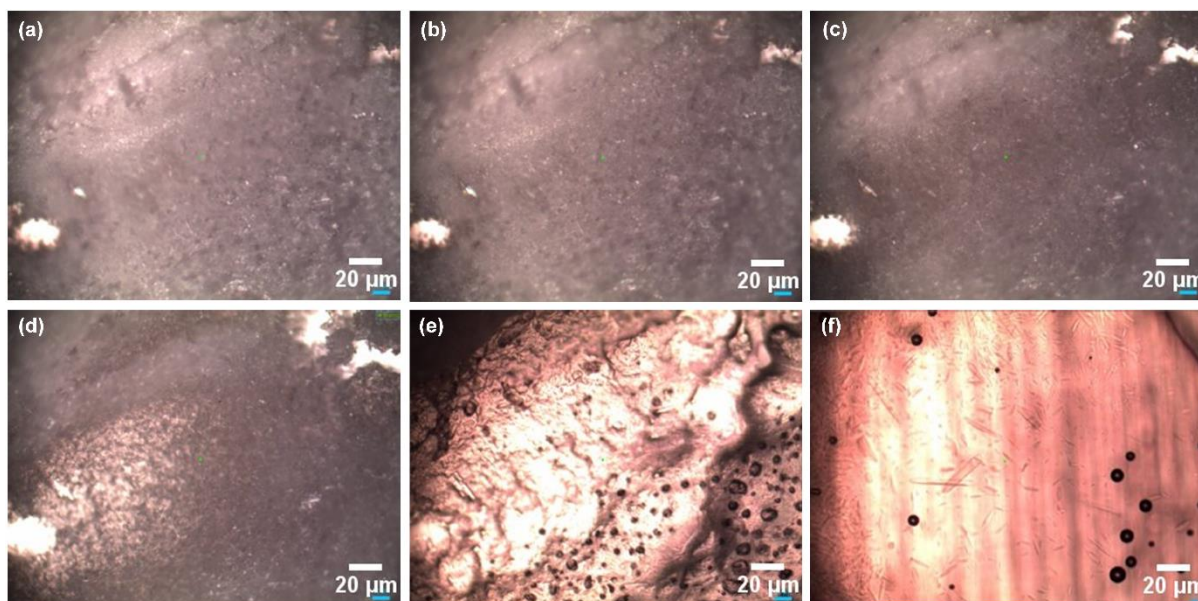


Figure 4. Optical micrographs of ramipril from hot-stage Raman spectrometer collected at different temperatures (a) at room temperature, (b) at 70°C after 30 min, (c) at 90°C after 5min, (d) at 105°C, (e) at 107°C, (f) at 108°C.

The significance of printing ramipril at lower temperatures is further explained by studying the behaviour of the ramipril melt during the cooling cycle. Ramipril was allowed to completely melt by heating the hot-stage to 109 °C and spectra were collected at different intervals during the cooling cycle of the melt. It was observed that the Raman spectra of the cooled material are different from that of crystalline ramipril. Splitting of the peak corresponding to the C = O functional group (in conjugation with the primary amide) observed in the frequency region of 1635-1665 cm^{-1} and the absence of the peak corresponding to the O-H functional group in the frequency region of 3200-3400 cm^{-1} were identified as the predominant differences in the cooled melt and ramipril as received (Figure 5). This can be explained by the possibility of degradation of ramipril to its impurity D during melting. Studies suggest that rampiril diketopiperazine (impurity D) can be synthesised by heating ramipril to 120 °C for up to 6 to 8 hr (Amjad Anwwari, 2008). The Raman spectra of impurity D synthesised by this method (Figure 7) was similar to that of the cooled melt of the ramipril (Figure 6). The absence of the carboxylic hydroxyl group and the presence of diketone (primary amide) functionality in the impurity D further corroborate the differences observed in the Raman spectra of the ramipril collected, before and after melting. This emphasises the need for processing ramipril at lower temperatures. These results also show

the potential of Raman spectroscopy as an in-line tool to monitor process induced transitions, even at low drug concentration (3% in this case). In-line monitoring would require preformulation experiments to prepare calibration curves and the application of chemometrics to analyse the Raman data. Demonstrations with two-dimensional (2D) printed formulations have been already reported using different drugs (Edinger et al., 2017).

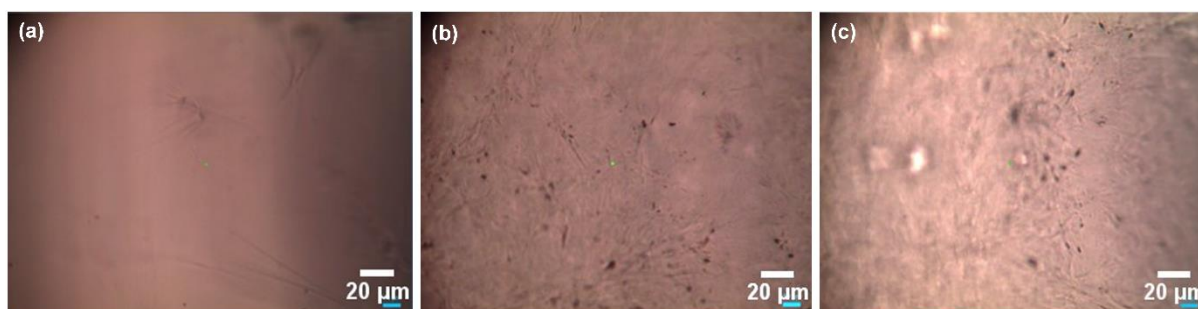


Figure 5. Optical micrographs of ramipril from hot-stage Raman spectrometer collected at different time intervals post-melting (a) after 5 min, (b) after 60 min, (c) after 180 min.

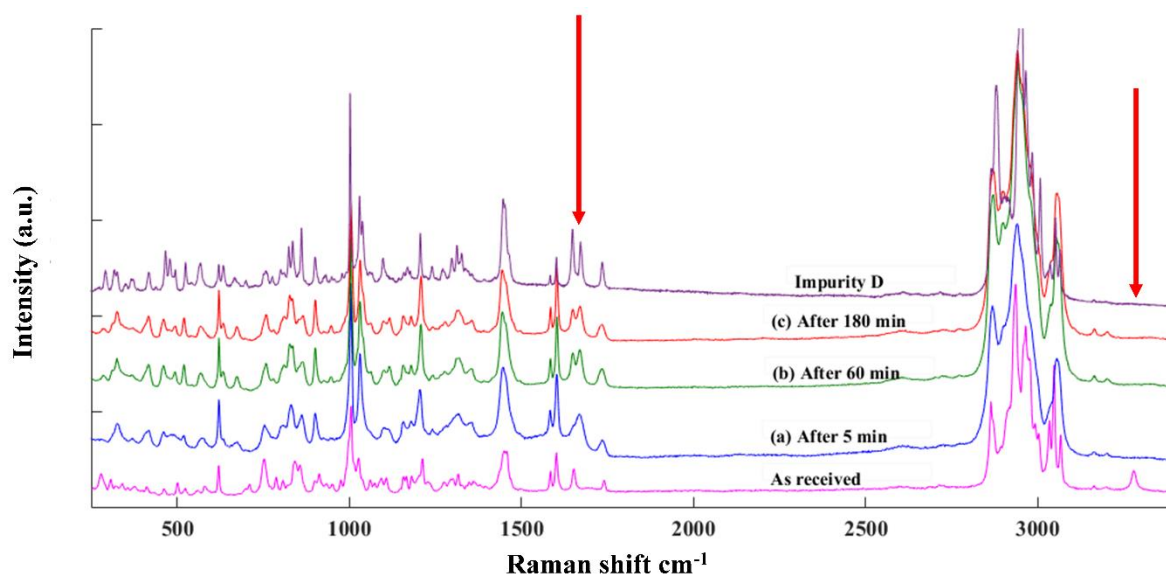


Figure 6. Raman spectra of ramipril collected at different time intervals post-melting (a) after 5 min, (b) after 60 min, (c) after 180 min, corresponding to images in the Figure 5.

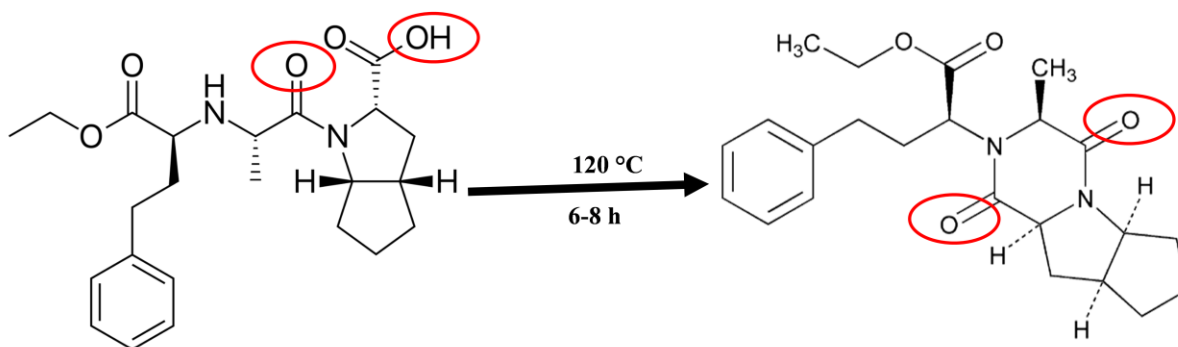


Figure 7. Schematic representation of synthesis of impurity D from ramipril, with marked functional groups, responsible for the differences in the Raman spectra.

Variable temperature SSNMR was used to support the results obtained from Raman spectroscopy. The SSNMR spectra of ramipril collected at temperatures used for extrusion and printing were similar to that of the ramipril at room temperature, except the broadening of the peaks observed in the chemical shift region 120-140 ppm (Figure 8), which possibly could be due to the molecular vibrations at higher temperatures. The spectrum collected after cooling the sample back to the room temperature (Figure 8) further corroborates the stable nature of ramipril over processing temperature range.

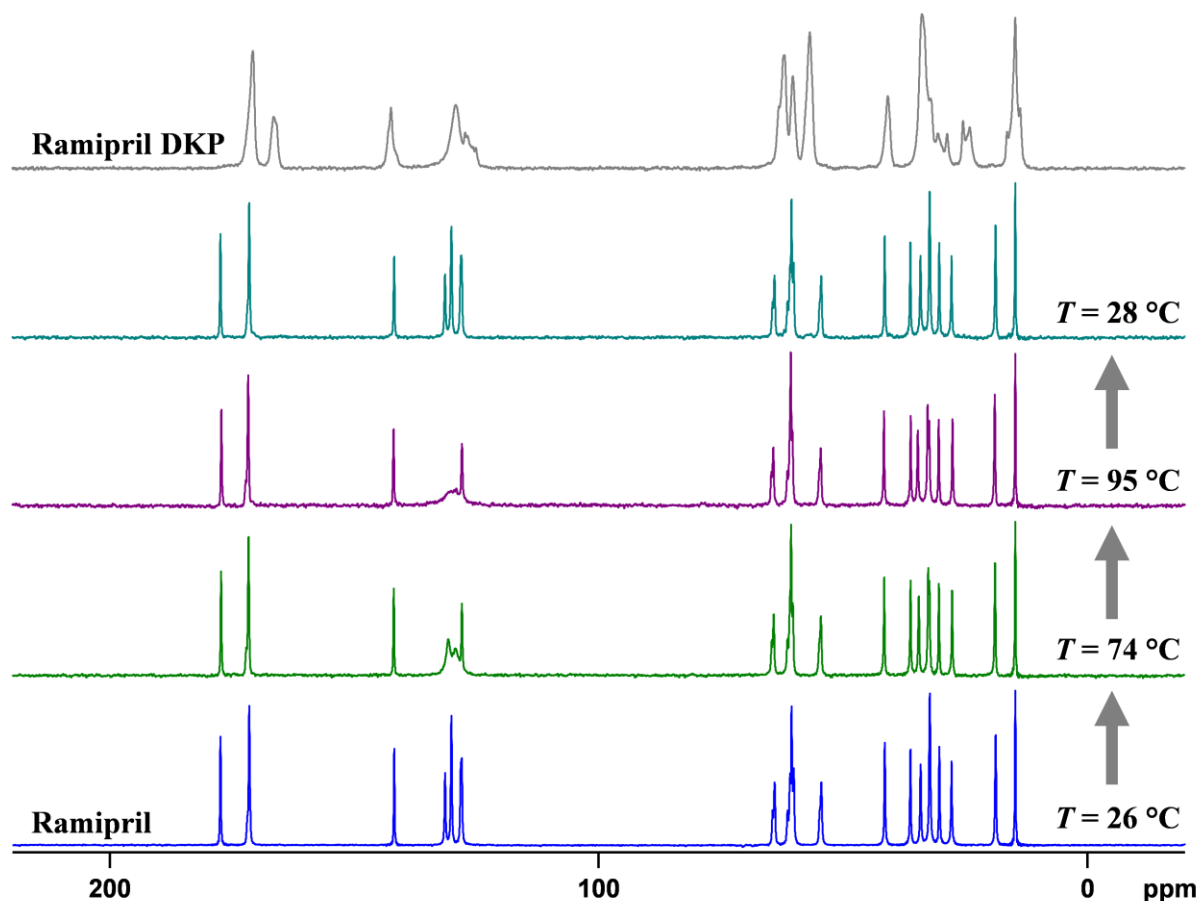


Figure 8. Experimental ^{13}C MAS NMR spectra of bulk crystalline ramipril under variable temperature conditions and of ramipril diketopiperazine (DKP) at ambient conditions. Spectra were acquired at $B_0 = 9.4$ T using the CP/TOSS pulse sequence with ^1H decoupling and from top to bottom consist of 1944, 243, 486, 486, and 1944 transients. The MAS frequency was 6 kHz for ramipril and 12 kHz for ramipril diketopiperazine. Temperatures shown are peak sample temperatures.

XRPD and SSNMR were used to examine the solid-state of the active ingredient in the final formulations. X-ray diffractograms of the pure components of the formulation were examined and the peaks corresponding to $2\theta^\circ$ - 7.6 and 8.11, were identified as the drug peaks without any interference from the excipient (Figure 9). The physical mixture of the formulation shows tiny peaks in this region indicating the crystalline nature of the drug but the powdered printlet does not show any peaks suggesting either the amorphous nature of the drug in the final formulation or the percentage of the drug is beyond the limit detection of the characterisation technique. Similar results were observed with SSNMR (Figure 10) where the physical mixture showed the presence of crystalline ramipril but the powdered printlet did not show any such signs, which again could possibly due to the amorphous nature of ramipril.

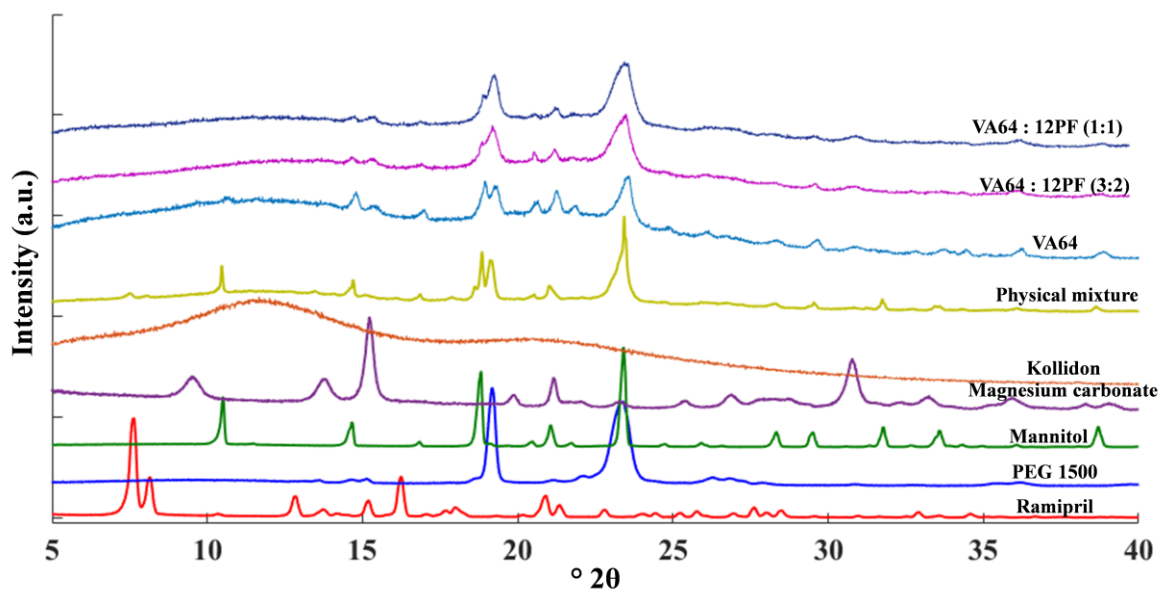


Figure 9. X-ray powder diffractograms of pure components, physical mixture before printing and powdered printlet of the three formulations.

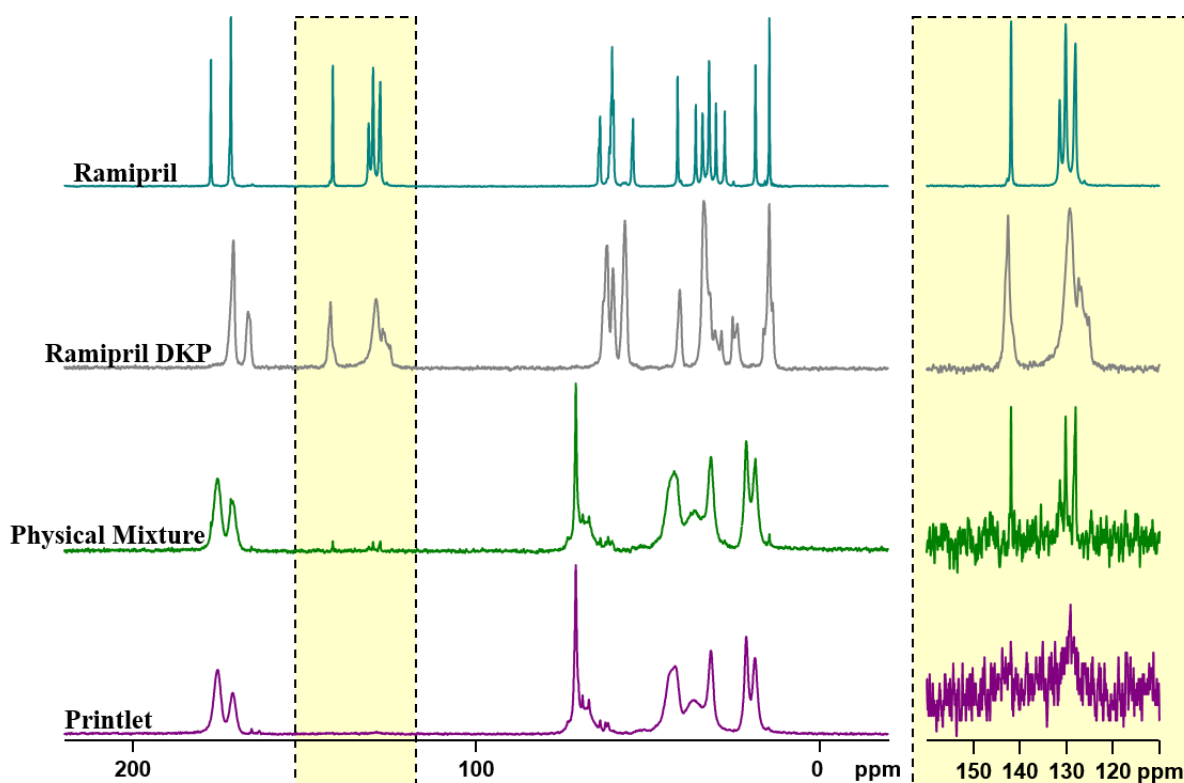


Figure 10. Experimental ^{13}C MAS NMR spectra of ramipril, ramipril diketopiperazine (DKP), extruded filament, and a physical mixture of the compounds comprising the filament. Spectra were acquired at $B_0 = 9.4$ T using the CP/TOSS pulse sequence with ^1H decoupling and consist of 4860, 1944, 7294, and 7294 transients, respectively. The MAS frequency was 12 kHz for all samples.

Having confirmed the applicability of Kollidon VA64 for FDM printing at lower temperature, additional filaments were also produced by replacing Kollidon VA64 entirely with Kollidon 12PF, while maintaining the rest of the formulation components constant. The extrusion process of this formulation was much smoother and efficient with an extrusion temperature of 65°C , which was lower than that used for Kollidon VA64. However these filaments were very brittle and not suitable for the subsequent printing steps. This could possibly be due to the lower molecular weight of the Kollidon 12PF which does not facilitate long range interlinking of the polymer chains, essential for the tensile strength of the filament. Taking into account the flexibility in filaments and ease of extrusion achieved using Kollidon VA64 and Kollidon 12PF respectively, filaments were produced using formulations where Kollidon VA64 was partly replaced by Kollidon 12PF (VA64:12PF in the ratios 3:2 and 1:1 as shown in Table 1). This resulted in production of filaments at a temperature of 65°C , which were suitable for printing at 90°C . XRPD and HPLC results of these formulations

were similar to that of the formulation VA64, showing drug stability during the printing process (data not shown).

Dissolution studies of all the three formulations were performed in 0.1N HCl, simulating gastric conditions as they were formulated with the objective of producing immediate release dosage form. Polymers themselves being water soluble, and with the low molecular weight water soluble components in the formulations acting as a pore formers, 100% drug release was achieved within 30 min across all the three formulations (Figure 11). Formulations containing Kollidon 12PF were observed to have an even faster drug release when compared to the one with Kollidon VA64 alone. This pattern is explained considering the extensive application of Kollidon 12PF as a solubility enhancer in pharmaceutical applications. From these observations, the mechanism of drug release from these Kollidon based FDM products could be explained by erosion.

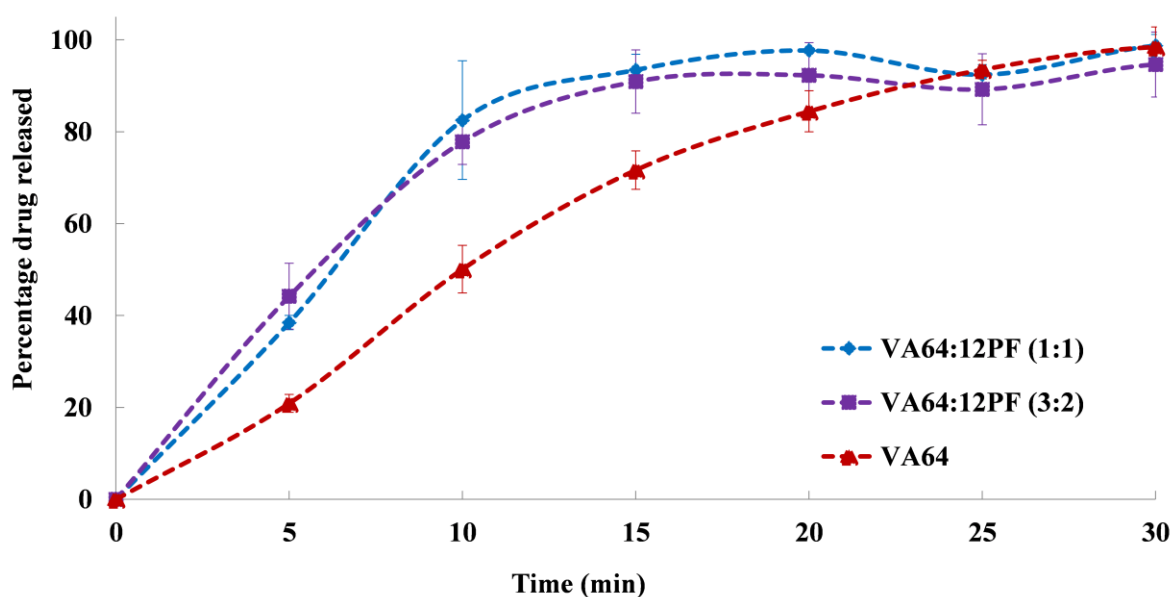


Figure 11. Dissolution profiles of ramipril printlets with a dose equivalent of 2 mg.

A previous study showed that 4-ASA when printed at temperatures generally used for FDM was degraded to approximately half of its initial dose (Goyanes et al., 2015a). To emphasise the significance of lowering the printing temperature in FDM, and as a probe that the selection of the right formulation composition could avoid degradation while printing, 4-ASA printlets were produced based on the formulation Kollidon VA64. The 4-ASA loaded Kollidon VA64 filaments were extruded at 75 °C and printed at 90°C. The evaluation of the drug content using HPLC showed a drug loading of the filaments of 2.91 wt% ± 0.02

(theoretical loading- 3 wt%) and the amount of drug in the final printlets was 2.05 ± 0.01 mg (theoretical amount- 2 mg). These results suggest that the drug did not undergo any degradation either during extrusion or printing, thereby validating the significance selecting polymers to print at lower temperatures.

Conclusion

The manufacture of ramipril printlets has been successfully demonstrated by FDM at 90 °C; the lowest printing temperature reported so far to the authors' knowledge. Kollidon VA64 as main polymer or in combination with Kollidon 12PF was used for the first time to produce immediate release printlets by FDM printing with no drug degradation. Kollidon 12PF printlets formulated in combination with VA64 showed a slightly faster dissolution profile when compared with those formulated with Kollidon VA64 alone. The applicability of these formulations to prepare low-melting temperature and thermolabile medicines by FDM printing has been demonstrated with the drugs ramipril and 4-ASA. This work demonstrates that the selection and use of new excipients can overcome drug degradation problems in FDM printing and thus, allows this technology to be suitable for thermolabile drugs.

Acknowledgements

This work has been financially supported by Science Foundation Ireland under the following grants: SSPC2 (12/RC/2275), Model Predictive Control of Continuous Pharmaceutical Processes (13/IA/1980) and Pharmaceutical Powder Extrusion Suite (12/RI/2345). Access to the 9.4 T solid-state NMR spectrometer was provided by the Bernal Institute at the University of Limerick (Limerick, Ireland). The SSNMR instrument is funded by a Programme for Research in Third-Level Institutions (PRTLII) cycle 5 award. SSNMR data were acquired, processed, and prepared for publication by Dr Alexandra Faucher.

References

- Alhnan, M.A., Okwuosa, T.C., Sadia, M., Wan, K.W., Ahmed, W., Arafat, B., 2016. Emergence of 3D Printed Dosage Forms: Opportunities and Challenges. *Pharm. Res.*
- Alomari, M., Mohamed, F.H., Basit, A.W., Gaisford, S., 2015. Personalised dosing: Printing a dose of one's own medicine. *Int. J. Pharm.* 494, 568-577.
- Amjad Anwwari, R.M., Sandeep Patil, Sudesh Bhure, N.P. Shetgiri, Anirudha Rakhe 2008. Synthesis and structural elucidation of impurities in ramipril tablets, <http://www.spectroscopyonline.com/synthesis-and-structural-elucidation-impurities-ramipril-tablets?id=&sk=&date=&pageID=3>, last accessed 15/03/2018.
- Ammann, C., Meier, P., Merbach, A., 1982. A simple multinuclear NMR thermometer. *Journal of Magnetic Resonance (1969)* 46, 319-321.
- Antzutkin, O., 1999. Sideband manipulation in magic-angle-spinning nuclear magnetic resonance. *Progress in nuclear magnetic resonance spectroscopy* 35, 203-266.
- Beck, R.C.R., Chaves, P.S., Goyanes, A., Vukosavljevic, B., Buanz, A., Windbergs, M., Basit, A.W., Gaisford, S., 2017. 3D printed tablets loaded with polymeric nanocapsules: An innovative approach to produce customized drug delivery systems. *Int. J. Pharm.* 528, 268-279.
- Bielecki, A., Burum, D.P., 1995. Temperature Dependence of ^{207}Pb MAS Spectra of Solid Lead Nitrate. An Accurate, Sensitive Thermometer for Variable-Temperature MAS. *Journal of Magnetic Resonance, Series A* 116, 215-220.
- Chia, H.N., Wu, B.M., 2015. Recent advances in 3D printing of biomaterials. *Journal of biological engineering* 9, 4.
- Edinger, M., Bar-Shalom, D., Rantanen, J., Genina, N., 2017. Visualization and Non-Destructive Quantification of Inkjet-Printed Pharmaceuticals on Different Substrates Using Raman Spectroscopy and Raman Chemical Imaging. *Pharm. Res.* 34, 1023-1036.
- Farrar, R.C., 1994. Fire resistant and high temperature insulating composition. Google Patents.
- Fina, F., Goyanes, A., Gaisford, S., Basit, A.W., 2017. Selective laser sintering (SLS) 3D printing of medicines. *Int. J. Pharm.* 529, 285-293.
- Fung, B., Khitritin, A., Ermolaev, K., 2000. An improved broadband decoupling sequence for liquid crystals and solids. *Journal of Magnetic Resonance* 142, 97-101.
- Goyanes, A., Buanz, A.B., Basit, A.W., Gaisford, S., 2014. Fused-filament 3D printing (3DP) for fabrication of tablets. *Int. J. Pharm.* 476, 88-92.
- Goyanes, A., Buanz, A.B., Hatton, G.B., Gaisford, S., Basit, A.W., 2015a. 3D printing of modified-release aminosalicylate (4-ASA and 5-ASA) tablets. *European Journal of Pharmaceutics and Biopharmaceutics* 89, 157-162.

- Goyanes, A., Buanz, A.B., Hatton, G.B., Gaisford, S., Basit, A.W., 2015b. 3D printing of modified-release aminosalicylate (4-ASA and 5-ASA) tablets. *Eur. J. Pharm. Biopharm.* 89, 157-162.
- Goyanes, A., Martinez, P.R., Buanz, A., Basit, A.W., Gaisford, S., 2015c. Effect of geometry on drug release from 3D printed tablets. *International journal of pharmaceutics* 494, 657-663.
- Goyanes, A., Wang, J., Buanz, A., Martinez-Pacheco, R., Telford, R., Gaisford, S., Basit, A.W., 2015d. 3D Printing of Medicines: Engineering Novel Oral Devices with Unique Design and Drug Release Characteristics. *Mol. Pharm.* 12, 4077-4084.
- Goyanes, A., Scarpa, M., Kamlow, M., Gaisford, S., Basit, A.W., Orlu, M., 2017. Patient acceptability of 3D printed medicines. *Int. J. Pharm.* 530, 71-78.
- Harris, M., Hokanson, G., Murthy, K., Reisch, R., Waldman, F., 1988. Stabilized compositions. Google Patents.
- Karl, M., Nalawade, S., Maschke, A., Djuric, D., Kolter, K., 2010. Suitability of pure and plasticized polymers for hot melt extrusion, The 37th Annual Meeting and Exposition of the Controlled Release Society. Portland: Oregon Convention Center.
- Khaled, S.A., Burley, J.C., Alexander, M.R., Yang, J., Roberts, C.J., 2015a. 3D printing of five-in-one dose combination polypill with defined immediate and sustained release profiles. *Journal of controlled release* 217, 308-314.
- Khaled, S.A., Burley, J.C., Alexander, M.R., Yang, J., Roberts, C.J., 2015b. 3D printing of tablets containing multiple drugs with defined release profiles. *International journal of pharmaceutics* 494, 643-650.
- Massiot, D., Fayon, F., Capron, M., King, I., Le Calvé, S., Alonso, B., Durand, J.O., Bujoli, B., Gan, Z., Hoatson, G., 2002. Modelling one-and two-dimensional solid-state NMR spectra. *Magnetic Resonance in Chemistry* 40, 70-76.
- Melocchi, A., Parietti, F., Loreti, G., Maroni, A., Gazzaniga, A., Zema, L., 2015. 3D printing by fused deposition modeling (FDM) of a swellable/erodible capsular device for oral pulsatile release of drugs. *Journal of Drug Delivery Science and Technology* 30, 360-367.
- Morcombe, C.R., Zilm, K.W., 2003. Chemical shift referencing in MAS solid state NMR. *Journal of Magnetic Resonance* 162, 479-486.
- Okwuosa, T.C., Stefaniak, D., Arafat, B., Isreb, A., Wan, K.-W., Alhnan, M.A., 2016. A lower temperature FDM 3D printing for the manufacture of patient-specific immediate release tablets. *Pharmaceutical research* 33, 2704-2712.
- Palo, M., Holländer, J., Suominen, J., Yliruusi, J., Sandler, N., 2017. 3D printed drug delivery devices: perspectives and technical challenges. *Expert Review of Medical Devices* 14, 685-696.
- Pietrzak, K., Isreb, A., Alhnan, M.A., 2015. A flexible-dose dispenser for immediate and extended release 3D printed tablets. *Eur. J. Pharm. Biopharm.* 96, 380-387.

Sachs, E.M., Haggerty, J.S., Cima, M.J., Williams, P.A., 1993. Three-dimensional printing techniques. Google Patents.

Sadia, M., Sośnicka, A., Arafat, B., Isreb, A., Ahmed, W., Kellarakis, A., Alhnan, M.A., 2016. Adaptation of pharmaceutical excipients to FDM 3D printing for the fabrication of patient-tailored immediate release tablets. *International journal of pharmaceutics* 513, 659-668.

Schiele, J.T., Quinzler, R., Klimm, H.-D., Pruszydło, M.G., Haefeli, W.E., 2013. Difficulties swallowing solid oral dosage forms in a general practice population: prevalence, causes, and relationship to dosage forms. *European journal of clinical pharmacology* 69, 937-948.

Shafiq, S., Shakeel, F., 2008. Enhanced stability of ramipril in nanoemulsion containing Cremophor-EL: a technical note. *Aaps Pharmscitech* 9, 1097-1101.

Skowrya, J., Pietrzak, K., Alhnan, M.A., 2015. Fabrication of extended-release patient-tailored prednisolone tablets via fused deposition modelling (FDM) 3D printing. *European Journal of Pharmaceutical Sciences* 68, 11-17.

Song, Z., Antzutkin, O.N., Feng, X., Levitt, M.H., 1993. Sideband suppression in magic-angle-spinning NMR by a sequence of 5π pulses. *Solid state nuclear magnetic resonance* 2, 143-146.

Takahashi, T., Kawashima, H., Sugisawa, H., Baba, T., 1999. ^{207}Pb chemical shift thermometer at high temperature for magic angle spinning experiments. *Solid State Nuclear Magnetic Resonance* 15, 119-123.

Trenfield, S.J., Awad, A., Goyanes, A., Gaisford, S., Basit, A.W., 2018. 3D Printing Pharmaceuticals: Drug Development to Frontline Care. *Trends Pharmacol. Sci.* 39, 440-451.

Warner, G.T., Perry, C.M., 2002. Ramipril. *Drugs* 62, 1381-1405.